

# **Transient Scuffing of Candidate Diesel Engine Materials at Temperatures up to 600°C**

Project Milestone Report

**March 2003**

**Peter J. Blau**

## **Transient Scuffing of Candidate Diesel Engine Materials at Temperatures up to 600°C**

March 31, 2003

prepared for

Dr. Sidney Diamond  
U.S. Department of Energy  
Office of FreedomCAR and Vehicle Technologies Program

by

Peter J. Blau, Jun Qu, and Ronald D. Ott  
Metals and Ceramics Division  
Oak Ridge National Laboratory  
P. O. Box 2008 – Mail Stop 6063  
Oak Ridge, TN 37831-6063

# CONTENTS

Summary of this Report .....	1
1.0 Introduction to Scuffing and its Basic Mechanisms .....	2
2.0 Scuffing Models.....	5
3.0 Scuffing-Related Parameters .....	7
4.0 Naturally-Formed Lubricous Layers in Scuffing-Critical Systems .....	8
5.0 High-Temperature Scuffing Studies at ORNL.....	9
5.1 Apparatus and Methodology .....	9
5.2 Material Rankings .....	9
5.3 Transient Torque Behavior and Mechanisms of Scuffing at High Temperature.....	10
6.0 Observations .....	15
7.0 Summary and Implications.....	16
8.0 Future Plans .....	17
References.....	18
List of Figures.....	19
Distribution List.....	20

## **Summary of this Report**

This milestone report summarizes the general characteristics of scuffing damage to solid surfaces, then describes transient effects on scuffing observed during oscillating sliding wear tests of candidate material pairs for high-temperature diesel engine applications, like waste-gate bushings in exhaust gas recirculation (EGR) systems. It is shown that oxidation and the formation of wear particle layers influence the friction of such components. In the case of metallic materials in cylindrical contacts where there is a generous clearance, debris layers can form which reduce the torque over time. For ceramic combinations, the opposite effect is observed. Here, the accumulation of wear debris leads to an increase in the turning torque. High-temperature transient scuffing behavior is considered in terms of a series of stages in which the composition and morphology of the contact is changing. These changes are used to explain the behavior of 11 material pairs consisting of stainless steels, Ni-based alloys, Co-based alloys, and structural ceramics.

## 1.0 Introduction to Scuffing and its Basic Mechanisms

The word *scuffing* is one of the most widely-used terms in the field of lubrication and wear. Common usage varies from the abrasion of leather, as in “Son, don’t scuff your new shoes!” to the description of damage that occurs on piston skirts, cylinder liners, fuel injector plungers, cam lobes, gear teeth, and other lubricated engine components. It is this latter application that has been the focus of research which seeks a better understanding of the conditions that lead to its onset and progression.

The term scuffing has been used in reports on engine lubrication and wear almost casually, without defining it, with the implication that the reader will understand the term from the context of daily experience. Yet, the process of reaching a consensus definition for the term scuffing has troubled the standardization community. In fact for a number of years, ASTM’s terminology standard G-40 listed scuffing as a deprecated term that should not be used due to its ambiguity. More recently, and only after considerable debate, the following definition evolved [1]:

**scuffing**, n. – a form of wear occurring in inadequately lubricated tribosystems that is characterized by macroscopically-observable changes in surface texture, with features related to the direction of motion. *Discussion* – Features characteristic of scuffing include scratches, plastic deformation, and transferred material. (Related terms: **galling**, **scoring**.)

Even this carefully-crafted definition may not reflect the range of common usage. In fact, the ASTM definition could also be applied to some forms of abrasive and adhesive wear, so it falls short of uniquely defining scuffing.

Cultural differences and the individual experience of researchers also create problems in defining and characterizing the scuffing phenomenon. The terms scoring and galling, used in the U.S., are sometimes replaced by the term scuffing in the United Kingdom [2]. In the ASME Wear Control Handbook [3], Godfrey seems to equate scuffing with sliding wear: “Severe adhesive wear or scuffing is recognized with the unaided eye by gross amounts of transferred material; rough, torn surfaces and plastic deformation; and large metallic wear fragments ...” Over a decade later, Martin described scuffing in the ASM Handbook as follows [4]: “Scuffing is related to failure of the lubricating film and is caused by over heating, which could be due to friction and the sliding velocity between surfaces.” Investigators like Barwell [5] have defined scuffing in terms of what happens after film breakdown. He said scuffing was “gross damage characterized by the formation of local welds between sliding surfaces.” If scuffing were equivalent to adhesive wear, why should it require a separate term? Clearly, there is an element of differentiation missing in most published descriptions.

Five features commonly associated with the scuffing of metallic engine parts are as follows:

- (1) Scuffing is usually attributed to the failure of a lubricating film to work properly. In addition, overloading, over-speed, particulate contaminants in the oil, and localized thermal excursions on an asperity level have been postulated as the causes for scuffing.

(2) Sufficient plastic deformation occurs on a contact surface to cause it to change its appearance to the naked eye. It becomes either shinier or duller than the original surface. Since polishing would produce such effects, is scuffing akin to polishing?

(3) Scuffing can occur without a net loss of material. Lateral displacement or smearing of surface material can occur without the creation of loose wear particles. If wear involves the progressive loss of material, then scuffing is not a form of wear.

(4) Scuffing tends to be localized, and some portions of a surface may remain pristine while others exhibit noticeable damage. This localization makes quantitative measurement of the degree of scuffing difficult.

(5) Scuffing can occur within the first few rubs or it may develop only after a longer period of rubbing contact.

(6) Scuffing is often associated with a relatively sudden increase in friction, but not so high that the tribosystem seizes.

Previous investigators have tied the effects of particulate contamination in oils with the occurrence of scuffing (e.g. [6,7]). However, the role of third-bodies in producing abraded areas of pistons was differentiated from scuffing by Cattaneo and Starkman [8] in a paper authored over half a century ago. They remarked: "Many of the cylinder failures reported as 'scuffing' are believed to have been due to 'surface disintegration.' ... a large part of the wear of cylinders is due to a mechanical breakdown of the surface which can occur without any initial breakdown of the lubricating oil film [that is characteristic of scuffing]." Surface disintegration was described as the production of tiny wear particles that became entrained within the lubricant film and abrade the surfaces so as to produce a scuffed appearance.

Investigators who try to understand the mechanisms of scuffing and develop models frequently include temperature as a variable. For example, attempts have been made to define a critical temperature at which a lubricating film breaks down, leading to a perceptible rise in friction force. But that approach may not be comprehensive enough to describe the behavior of formulated lubricants. Rather, Enthoven, et al. [9] observed that well-formulated oils contain additive packages whose constituents not only affect the load carrying capabilities (viscosity) of the lubricant, but also react with bearing surfaces to create lubricious or wear-reducing boundary layers. Thus, the process that leads to scuffing must not only degrade the hydrodynamic characteristics of the oil film, but also break down the chemically-reactive surface films whose formation is facilitated by a rise in surface temperature. Consequently, a knowledge of the local surface temperature becomes important in treating such cases.

Since defining the characteristics of scuffing fails to reach a consensus among users of the term, it is unrealistic to expect that a single mechanistic model for scuffing will satisfy the needs of the entire tribology community. Rather, the context of any scuffing model must be limited in applicability. In the present case, we shall define scuffing in terms of a sequence of morphological and microstructural changes in a surface that eventually results in a degradation or loss of tribological function. For example, a change in clearance occurs between lubricated

mating parts, and there is a clear and perceptible rise in friction force associated with relatively small changes in the surface finish of the scuffed part.

There is no need for the progressive loss of material during scuffing, because a change in clearance could be caused by material displacement rather than by clogging with wear particles or the transfer of third bodies. However, the wide usage of the term scuffing does not preclude the possibility for wear.

## 2.0 Scuffing Models

From the ASTM definition, any scuffing model must include variables that are known to bring about the onset of macroscopically-observable surface damage. Confining the model to contain only mechanical or thermal or chemical variables would unreasonably limit its ability to depict the affects of relevant variables. Therefore, it was useful to list the potential variables as well as consider the magnitudes of their effects found by other investigators.

Fig. 1 portrays the problem in general terms. There are two solids, A and B, moving relative to one another under a non-zero normal force. The solids have, in the general case, different surface roughness. The instantaneous contact distribution is a stochastic process, dependent on the evolving surface topography. Depending on the composition of the lubricant and the temperature, there may be reaction films on A or B, or both A and B, and these films may or may not have the same composition. A liquid film separates the solids at most, but not all points on the surface. At some locations, the film may be squeezed out or excluded by wetting considerations. At any instant, the two solid bodies may be in contact, either directly or via the boundary films on one or both surfaces (for example, at points labeled “C”). The temperature at points C is likely to be momentarily greater than the mean temperature of the bulk material below and on either side. Wear particles or external contaminants may also be present.

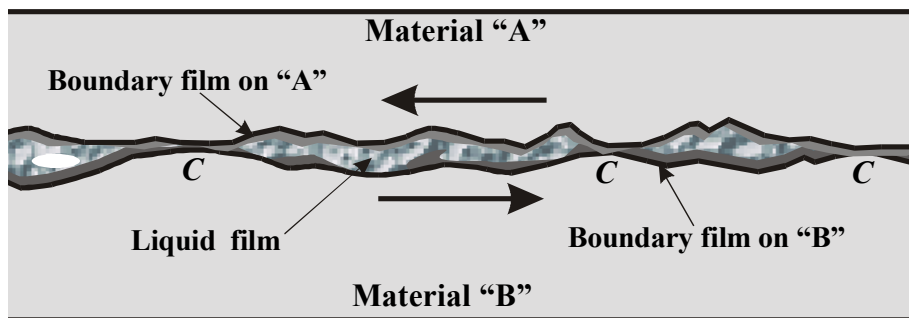


Fig. 1. Surfaces of two solids, containing boundary films, are moved relative to one another in the presence of a liquid lubricating film.

It is well-known that when the surfaces of the two bodies are first brought into contact, and if relative motion has not yet begun, a quasi-static situation will exist such that the highest interacting asperities will immediately deform to create sufficient area to support the load [10]. The total contact area created will be proportional to the hardness (yield pressure) of the softer of the two solids. At least some of the material will have been plastically deformed because the pressure at the first touching asperities will be very large. Adhesion may take place if the load induces a stress large enough to force the materials into intimate contact; however, in practical engineering systems containing oxide films and other interfacial species, immediate adhesion between Materials A and B is not assured.

When a tangential force is applied and relative motion begins, strong shear forces will be developed below the initial contact points. As these first contacts are broken and new sets of



contacts are made, the localized shear distribution from point-to-point on the surface will be in a continual state of change. The pattern and shapes of these localized shear points will be dependent on the roughness and lay (directionality of texture) of the two rubbing surfaces. If the contact geometry of the tribosystem enables a full lubricating film to form, the surfaces will lift off and scuffing will be delayed. But, as is the case for many practical systems in which the relative velocity changes periodically, there will be instances of contact between the reaction films or the solids, enabling elastic or plastic deformation to occur. At the same time, tribochemical reactions may be producing reaction products.

From a more macroscopic point of view, scuffing can be promoted or accelerated when the components are misaligned such that the load that is intended, by design, to be born by a larger surface is instead supported by a small fraction of the surface. Fig. 2 shows an exaggerated example of this situation for a cylindrical shaft, such as that in a valve guide, waste gate bushing, or fuel injector, with a slight axial misalignment, producing a force couple at opposite ends of the bore. That kind of problem can be solved by improving the manufacturing process to improve the fit, redesigning or adjusting to reduce the component misalignment, or substituting materials, surface treatments, or coatings that are more tolerant to higher localized contact loads.

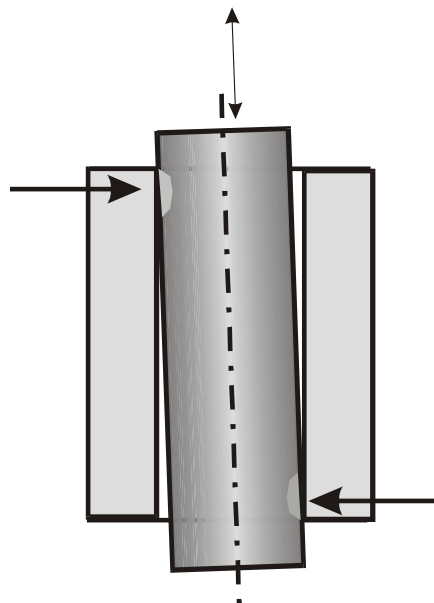


Fig. 2. Axial misalignment of an oscillating shaft can concentrate the stresses and result in an acceleration of scuffing at the upper and lower ends.

### 3.0 Scuffing-Related Parameters

Several parameters have been useful in modeling and understanding the mechanical portions of tribological contacts. In addition to the well-known equations of Hertz [11], which describe elastic contact of homogenous solids, the film thickness parameter,  $\Lambda$ , and the plasticity index,  $\psi$ , have been used for lubrication-related studies and for asperity deformation modeling, respectively. The film thickness parameter expresses the degree of interference between the composite surface roughness of both bodies [12], thus

$$\Lambda = \frac{h}{\sqrt{\sigma_1^2 + \sigma_2^2}} \quad [1]$$

where  $h$  = the mean lubricant film thickness, and  $\sigma_{1,2}$  is the root mean square surface roughness of the surfaces of the opposing bodies. When  $\Lambda < 3.0$  some degree of surface contact is expected, and the lower the  $\Lambda$  value, the less effective the lubricant in separating the surfaces under the applied conditions.

The plasticity index for a rough surface is a measure of the extent of plastic deformation of a set of normally-distributed asperities. It was introduced by Greenwood and Williamson [13] and then modified by Whitehouse and Archard [14],

$$\psi = \left( \frac{E'}{H} \right) \left( \frac{\sigma^*}{\beta} \right)^{1/2} \quad [2]$$

where  $H$  = the hardness of the surface,  $\sigma^*$  = the standard deviation of asperity heights,  $\beta$  = a correlation distance that is a function of the asperity size and height distribution, and  $E'$  is determined from  $E$  = the elastic modulus and  $\nu$  = Poissons ratio of the deforming surface as follows

$$E' = E (1 - \nu) \quad [2a]$$

Both the film thickness parameter and the plasticity index can change during running in. Therefore, scuffing condition maps such as those constructed by Hirst and Hollander [15] may represent, in general, only one instant of time in the life of a sliding contact – usually the beginning of contact, if they are based on measurements of initial, as-finished surface roughness values and quasi-static arguments.

#### **4.0 Naturally-Formed Lubricous Layers in Scuffing-Critical Systems**

While conventional forms of scuffing are associated with the failure of a liquid lubricant, there are special cases in which the failure of naturally formed solid films can also result in scuffing damage. An example of this phenomenon is provided by the formation of an oxide layer on a metal at high temperature. This layer can behave similarly to a solid lubricant until it becomes mechanically damaged during sliding contact. In that case, even non-liquid-lubricated contacts can experience effects akin to scuffing. Therefore, we shall refer to certain features of our high-temperature sliding contact test specimens as being scuffed.

## 5.0 High-Temperature Scuffing Studies at ORNL

**5.1 Apparatus and Methodology.** A specialized apparatus was built to study oscillating contact at temperatures up to and above  $600^{\circ}\text{C}$ , which is the thermal environment characteristic of exhaust valves and waste gate bushings in EGR systems. A schematic representation of the apparatus is shown at the left in Fig. 3. The details of the apparatus and cylinder-on-flat geometry have been described in a previous milestone report (Feb. 28, 2001), quarterly reports, and in a poster presented at the 2001 International Conference on Wear of Materials, Vancouver, Canada. One of the lower (flat) test specimens, displaying a characteristic “bow-tie” shaped wear scar is shown at the right of Fig. 3. For reference, the center hole is 6.35 mm ( $1/4"$ ) in diameter.

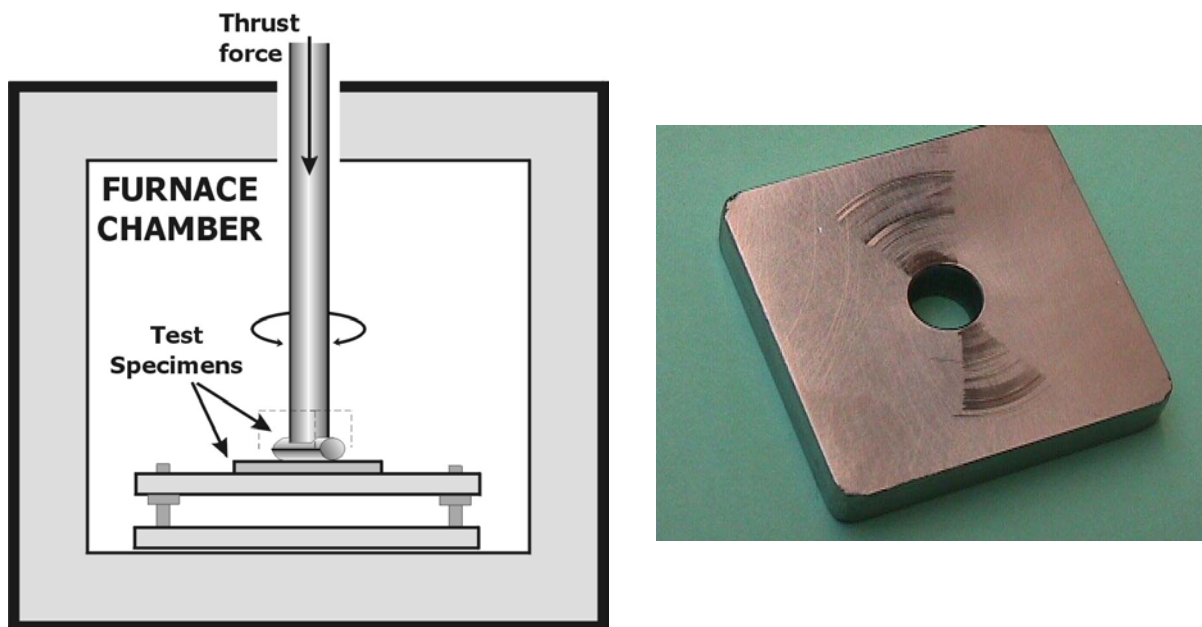


Fig. 3. Diagram of the high temperature scuffing test apparatus (left), and a representative lower test specimen of 304 stainless steel showing a non-uniform scuffing pattern (right).

After exploratory trials, the final test parameters were established. The normal force was 10 N, and the oscillating rate was 1 Hz at  $600^{\circ}\text{C}$  in air. At a cycle rate of 1 Hz, 60 minutes of testing produced 3600 full cycles of oscillation. Torque readings were taken at start-up, then at 10 minute intervals to study transient behavior.

**5.2 Material Rankings.** In addition to torque measurements, several criteria were used to rank the performance of the 10 material pairs in the test matrix. The best ranking in each category was used to normalize the other values to a maximum score of 100. The best received 100 and the others were a fraction of that. On this basis, the results of the high-temperature scuffing test matrix, including the two most recently evaluated material pairs, are given in Table 1.

**Table 1. Weighted Rankings of High-Temperature Scuff Test Pairs**  
[Top score in each category is in **bold face font**]

Pin	Tile	Index 1	rating 1	Index 2	rating 2	Index 3	rating 3	Index 4	rating 4	Index 5	rating 5	Index 6	rating 6	Sum
St6	P80	120.57	47.8	33.92	35.2	46.25	71.6	17.21	57.5	0.33	9.1	4.70	6.8	227.9
Zr	304	107.57	53.6	28.36	42.1	69.48	47.6	16.25	60.9	0.18	16.7	4.14	7.7	228.5
St6	304	116.78	49.3	32.40	36.8	58.81	56.3	13.73	72.0	0.16	18.8	5.62	5.7	238.9
303	304	99.35	58.0	27.06	44.1	45.01	73.5	12.35	80.1	2.70	1.1	4.15	7.7	264.5
T20	IC	73.24	78.7	13.66	87.3	44.95	73.6	14.41	68.6	0.11	27.3	0.90	35.6	371.1
Zr	SN	95.04	60.6	19.32	61.7	96.18	34.4	48.58	20.4	<b>0.03</b>	<b>100.0</b>	<b>0.32</b>	<b>100.0</b>	377.2
St6	465	58.76	98.1	13.23	90.2	47.77	69.3	18.89	52.4	0.04	75.0	2.05	15.6	400.5
St6	IC	80.84	71.3	13.14	90.8	41.93	78.9	10.18	97.2	0.09	33.3	0.88	36.4	407.9
GT	GT	<b>57.63</b>	<b>100.0</b>	14.54	82.0	<b>33.10</b>	<b>100.0</b>	10.35	95.6	0.15	20.0	2.62	12.2	409.8
Zr	IC	74.36	77.5	<b>11.93</b>	<b>100.0</b>	41.48	79.8	<b>9.89</b>	<b>100.0</b>	0.05	60.0	0.73	43.8	<b>461.1</b>

Material codes:

St6 = Stellite 6B, 303SS = 303 stainless steel, 304SS = 304 stainless steel, GT = GallTough stainless, Zr = TTZ zirconia, IC = alloy IC 221M, 465 = Custom 465 alloy, SN = silicon nitride type GS-44 (hot isopressed), P80 = Pyromet 80 alloy, T = Tribonic 20 alloy

Table Index codes:

(1) Average of initial torque (N-mm)

(2) Standard deviation in initial torque (N-mm)

(3) Average of final torque (N-mm)

(4) Standard deviation in final torque (N-mm)

(5) Pin specimen wear volume (mm<sup>3</sup>)

(6) Tile specimen roughness, Ra (μm)

Overall, the combination of zirconia on IC 221M intermetallic alloy provided the highest rating (461). Note that the transformation-toughened zirconia (TTZ) on silicon nitride couple gave the best wear behavior, but the final torque values (Indexes 3 and 4) were the worst of any couple. The new combinations tested this period (Stellite 6B on heat-treated Pyromet 80 and Stellite 6B on heat-treated Custom 465) did not perform better than the leading material combinations that were evaluated during the previous quarters.

*5.3 Transient Torque Behavior and Mechanisms of Scuffing at High Temperature.* The measured torque values, sampled at prescribed intervals, reflect the changing state of the interface and can serve as an indication of the initiation of scuffing damage and its transition into more severe forms of wear. Average torque, sampled at 5 minutes intervals by a data-acquisition system, are shown in Fig. 4 for two baseline tests with a stainless steel 303 pin on a stainless steel 304 flat specimen (600° C). For comparison, similar torque data for self-mated GallTough, a surface damage-resistant stainless steel, are shown in Fig. 5. In addition, a proprietary, zirconia-containing coating (from C3 Technologies, Georgia) was applied on the upper pin in one test, but as Fig. 5 data indicate, did not reduce the torque in these tests. Data in Fig. 5 show a trend for torque to decrease with time. Comparing the two material pairs, the 303/304 couples started at higher initial values than GallTough, but tended toward a similar ending value.

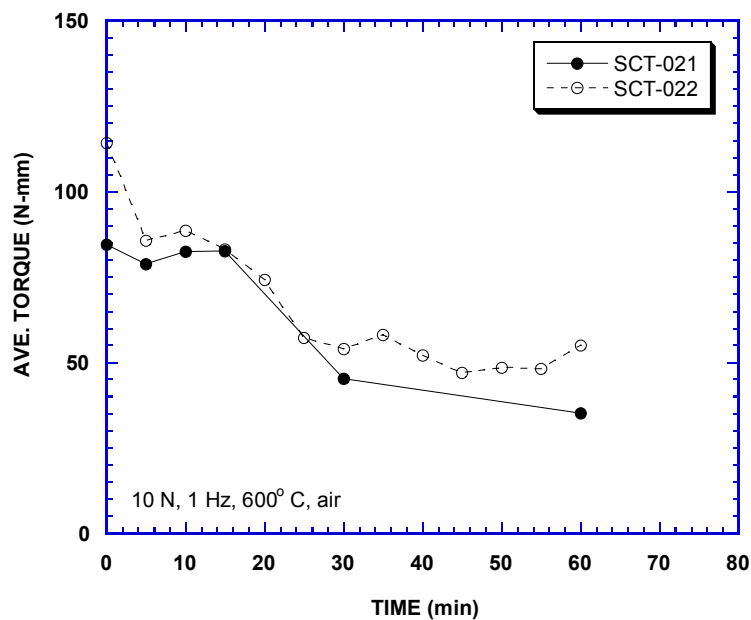


Fig. 4. Torque history for a baseline pair of stainless steel (303 on 304).

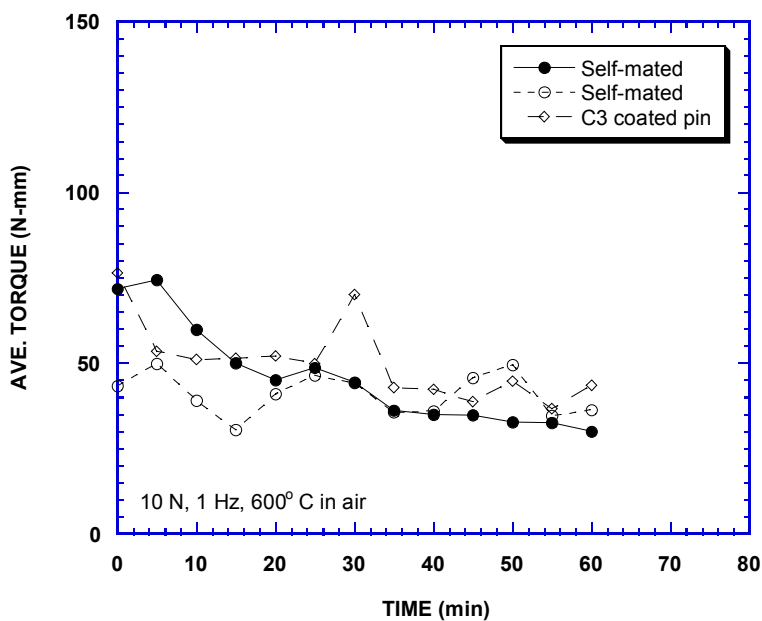


Fig. 5. Comparison of torque data for self-mated GallTough with a pair containing a coated pin.

Fig. 6 summarizes the torque histories for tests that used Co-based alloy Stellite 6B as the upper pin specimen, but various materials for the lower specimen. Two tests results are plotted for

each flat specimen material. The baseline, 304 stainless steel had the highest torque. The Custom 465, an Fe-based 12 wt% Cr, 11 wt% Ni alloy, had the most stable, lowest torque.

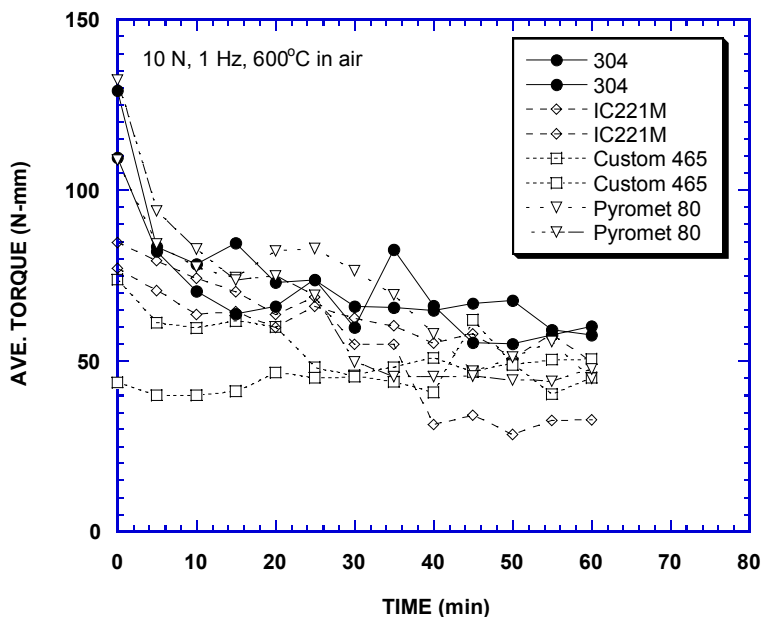


Fig. 6. Torque histories of various lower specimen materials against Stellite 6B pins.

Material couples containing zirconia as the test pin generally performed worse in torque behavior than the metallic alloys with one notable exception (Fig. 7). The couple containing zirconia on intermetallic alloy IC 221M had the lowest torque results of any couple tested. For the metallic couples, the torque reduction with time apparently corresponded to the build-up of a layer of wear particles, mainly oxidized metallic fragments (as in the example in Fig. 8). That layer serves two purposes: (1) to reduce the shear strength of the interface by creating a granular coating, and (2) to decrease the contact pressure in the interface by creating a cushion. For the zirconia-on-silicon nitride couples, the abrasive ceramic wear particles produced would have been less benign than a soft layer of mixed metal flakes and oxides. Since the ceramic wear debris did not behave as a shearable cushion it did not result in a decrease in torque as the debris built up.

The mechanism by which the IC221M  $\text{Ni}_3\text{Al}$  based alloy was able to maintain a lower torque against the zirconia was not so obvious. That behavior cannot be simply explained in terms of the build-up of an oxide debris layer since that would have also caused the torque for the 304 material to decrease with time as well (c.f. Fig. 7). Rather, it was instructive to consider all the couples containing IC 221M alloy (see Fig. 9). In all cases, including the zirconia-containing couple, those pairs showed a relatively steady decline. The average torque for all TTZ pairs, indicated by the solid line, can be fitted to a second-degree polynomial, as indicated in Fig. 9.

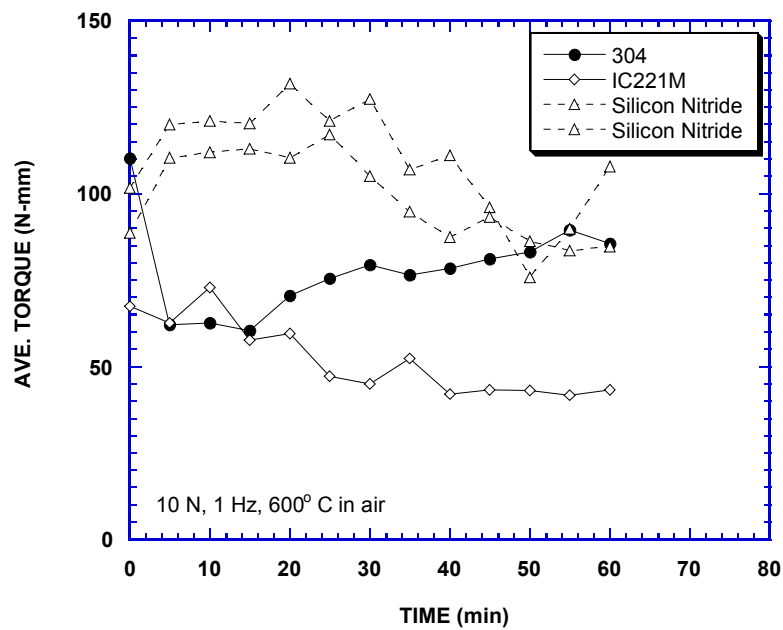


Fig. 7. Summary of torque histories for zirconia pins against three flat specimen materials.

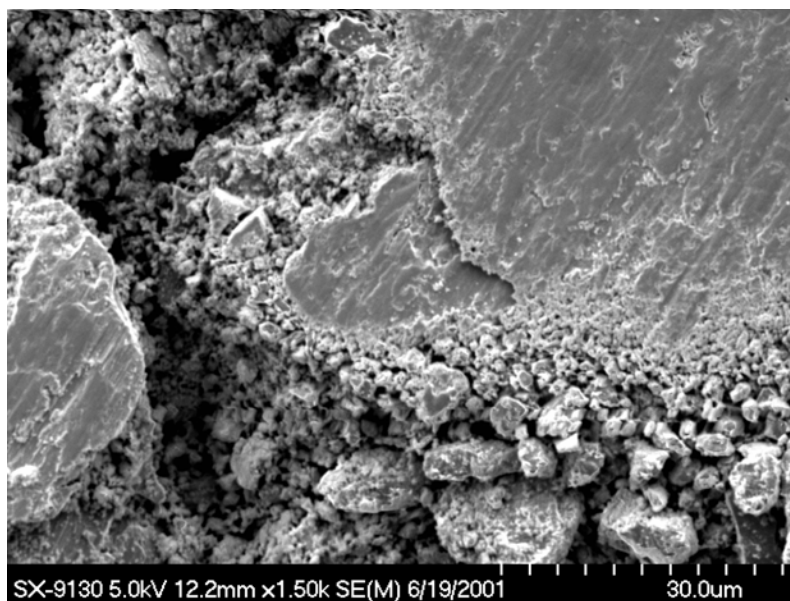


Fig. 8. Compressed debris layer formed from a 600° C test on 304 stainless steel.



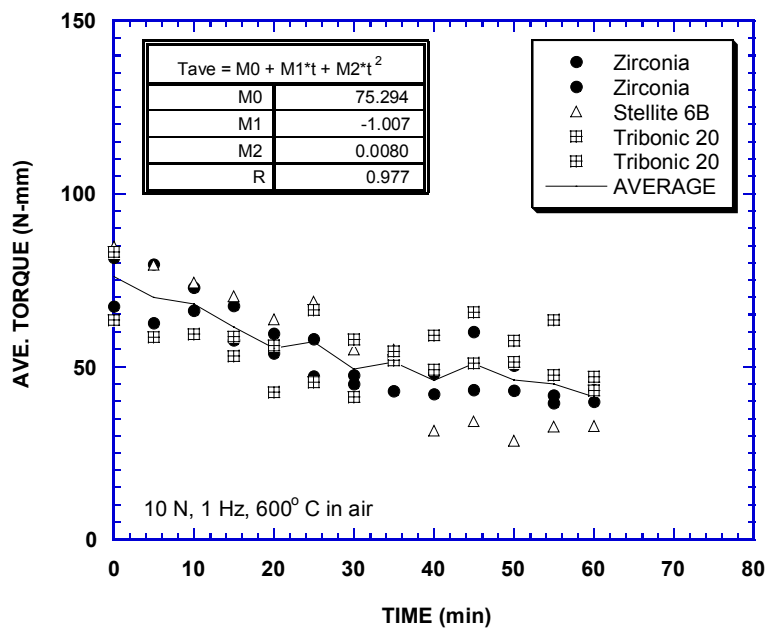


Fig. 9. Comparison of torque histories for all pairs in which IC 221M was the flat specimen.

## 6.0 Observations

Except in the case of ceramic on ceramic where the surface damage was very localized and produced little evidence for wear, these high-temperature scuffing results showed clear evidence for the importance of wear particles. Optical and scanning electron microscopy indicated the presence of both loose and compressed debris on most tile and pin specimens. Transients in scuffing behavior were associated with the disruption of the initial surfaces, creation of debris layers, and the role of those layers in both supporting the load and reducing the shear strength of the contact.

Based on observations on the variability of torque transients, the roughening of surfaces, and the formation of third-body layers, the sequence of stages undergone during the course of testing for metallic alloys can be summarized as follows:

1. Oxidation of the specimens as temperature rose
2. High initial contact stress (unworn specimens) causing a disruption of any initial lubricious oxide films that formed under ambient conditions, and during heat-up, progressive scuffing, and the rapid wear-in of one or both surfaces to produce third-bodies.
3. Agglomeration and development of layers of mixed oxide particles and wear debris.
4. Periodic layer loss and reformation causing momentary transients in torque response.

The foregoing scenario would be similar for the ceramics, however, the oxide layer effects would not have come into play, and micro-fracture would create a different type of debris layer, with less beneficial effects on torque reduction – especially with two ceramics in the pair.

Implications are that torque reduction by debris could only occur if there was enough clearance in the component (cylindrical shaft in a bushing) to enable such layers to form. If the clearance was too small, the formation of debris from disrupted oxide films might lead to seizure. This suggests using a surface texture to enable a friction-reducing debris layer to form, yet still provide channels for any excess debris to be removed from the contact. Very tight-fits of sliding components at high temperatures would probably not work well in the presence of the types of phenomena observed in these experiments.

## 7.0 Summary and Implications

Scuffing has been variously defined in the tribology literature, but the phenomena that comprise it are normally associated with the failure of liquid lubricated contacts. In the present context, scuffing-like behavior can be observed in elevated temperature sliding contacts where oxides become factio lubricating layers, soon to be disrupted by scuffing which leads to more debris production and the formation of third-body layers that reduce the level of friction. Transient behavior results in a progression of surface altering stages, tending to produce similar frictional response for almost all test when they approach 3600 cycles of oscillation.

Material couples containing the intermetallic alloy IC 221M seem to exhibit lower torques than others, and the zirconia/IC 221M couple was best in terms of torque. Of the more common commercial alloys, Custom 465 against Stellite 6B also showed low and more stable torque characteristics.

Applications like valve guides require the compromise of a close fit to ensure sealing, yet still provide a means for lubricant and enter. In other applications, like EGR waste-gate bushings, the possibility to account for lubrication with oxides and fine debris might be considered. If too much debris is generated, however, clogging of the bore may occur; however, a small amount of mixed oxide debris distributed on the contacting interface may provide a lubrication effect, as the present experiments suggest. In any case, the presence of scuffing transients makes it unlikely that a constant level of surface finish and torque behavior can be maintained in high-temperature sliding components over their operating lifetimes unless designers succeed in optimizing the macrocontact configuration, the correct material pairs, and the surface finish and lay to help manage third-bodies that are generated during scuffing and subsequent wear.

## 8.0 Future Plans

Work to link the composition and microstructures of engine materials with their scuffing characteristics continues under the project “*Durability of Diesel Engine Components*.” A report on the application of scanning acoustic microscopy to the analysis of surface contact damage is currently in preparation. It will describe how acoustic imaging can help in the study of high-temperature scuffing behavior using the specimens generated in the experiments mentioned here.

## References

- [1] ASTM Standard G-40-01, "Standard Terminology Relating to Erosion and Wear," Annual Book of Standards, Vol. 03.02 (2000) p. 166.
- [2] H. Blok, "Gear Wear as Related to the Viscosity of Oil," in Mechanical Wear, ed. J. T. Burwell, Jr., American Society of Metals, Ohio (1950) pp. 199-277.
- [3] D. Godfrey, "Diagnosis of Wear Mechanisms," in Wear Control Handbook, ed. W. O. Winer and M. B. Peterson, Amer. Soc. of Mech. Engineers, New York (1980) pp. 283-311.
- [4] H. Martin, "Vibration Analysis," in Friction, Lubrication, and Wear Technology, Vol. 18, ASM Handbook, ed. P. J. Blau, ASM International, Materials Park, Ohio (1992) pp. 293-298.
- [5] F. T. Barwell, "A Report on the Papers on Wear," *Proc. Instit. of Mech. Engineers*, Vol. 4 (1957) pp. 587-601.
- [6] S. Chandrasekaran, M. V. Khemchandani, and J. P. Sharma, "Effect of abrasive contaminants on scuffing," *Tribology International*, Vol. **18**(4), (1985) pp. 219-222.
- [7] S. Odi-Owei and B. J. Roylance, "The Effect of Solid Contamination on the Wear and Critical Failure Load in a Sliding Lubricated Contact," *Wear*, Vol. **112** (1986), pp. 239-255.
- [8] A. G. Cattaneo and E. S. Starkman, "Fuel and Lubrication Factors in Piston Ring and Cylinder Liner Wear," in Mechanical Wear, ed. J. T. Burwell, Jr., American Society of Metals, Ohio (1950) pp. 47-72.
- [9] J. C. Enthoven, P. M. Cann, and H. A. Spikes, "Temperature and Scuffing," *Tribology Trans.*, Vol. **36** (2) (1993) pp. 258-266.
- [10] F. P. Bowden and D. Tabor, The Friction and Lubrication of Solids, Oxford Press, UK (1950).
- [11] H. Hertz, "On the contact of solids," *J. Reine Angew. Math.*, Vol. **92** (1881) pp. 156-171.
- [12] M. M. Khonsari and R. R. Booser, Applied Tribology – Bearing Design and Lubrication, John Wiley and Sons, NY (2001) pp. 80-81.
- [13] J. A Greenwood and J. P. B. Williamson, "Contact of Nominally Flat Surfaces," *Proc. Royal Soc. of London*, Vol. **A295** (1966) pp. 300-319.
- [14] D. J. Whitehouse and J. F. Archard, "The properties of random surfaces of significance in their contact," *Proc. Royal Soc. of London*, Vol. **A316** (1970) pp. 97-121.
- [15] W. Hirst and A. E. Hollander, *Proc. Royal Soc. of London*, Vol. **A337** (1974) 379.

## List of Figures

Fig. 1. Surfaces of two solids, containing boundary films, are moved relative to one another in the presence of a liquid lubricating film. ....	5
Fig. 2. Axial misalignment of an oscillating shaft can concentrate the stresses and result in an acceleration of scuffing at the upper and lower ends. ....	6
Fig. 3. Diagram of the high temperature scuffing test apparatus (left), and a representative lower test specimen of 304 stainless steel showing a non-uniform scuffing pattern (right). ....	9
Fig. 4. Torque history for a baseline pair of stainless steel (303 on 304). ....	11
Fig. 5. Comparison of torque data for self-mated GallTough with a pair containing a coated pin. ....	11
Fig. 6. Torque histories of various lower specimen materials against Stellite 6B pins. ....	12
Fig. 7. Summary of torque histories for zirconia pins against three flat specimen materials. ....	13
Fig. 8. Compressed debris layer formed from a 600° C test on 304 stainless steel. ....	13
Fig. 9. Comparison of torque histories for all pairs in which IC 221M was the flat specimen. ....	14

## **INTERNAL DISTRIBUTION**

- |                                  |  |
|----------------------------------|--|
| 1. T. M. Besmann                 | 14. J. J. Truhan, Jr. (U of Tennessee) |
| 2 – 6. P. J. Blau                | 15. J. B. Green (NTRC)                 |
| 7 – 11. D. R. Johnson (5 copies) | 16. Central Research Library           |
| 12. A. E. Pasto                  | 17. ORNL Laboratory Records – RC       |
| 13. J. Qu                        | 18. ORNL Laboratory Records - OSTI     |

## **EXTERNAL DISTRIBUTION**

19. S. Diamond, U.S. Department of Energy, Office of FreedomCAR and Heavy Vehicle Technologies, EE 2G, 1000 Independence Ave. SW, Washington, DC 20585.
20. J. Routbort, Argonne National Laboratory, Bldg 212, 9700 S. Cass Avenue, Argonne, IL 60439.
21. George Fenske, Argonne National Laboratory, Bldg 212, 9700 S. Cass Avenue, Argonne, IL 60439.
22. L. Ojayi, Argonne National Laboratory, Bldg 212, 9700 S. Cass Avenue, Argonne, IL 60439.
23. David Cusac, Caterpillar Inc., Tech. Center-E/854, P. O. Box 1875, Peoria, IL 61656-1875
24. Larry Seitsman, Caterpillar Inc., Tech. Center, P. O. Box 1875, Peoria, IL 61656-1875
25. Simon Tung, General Motors (Mail Code: 480-106-160), CES Lab, RMB-194, 30500 Mound Road, Warren, MI 48090-9055
26. Valery Dunaevsky, Bendix Commercial Vehicle Systems, 901 Cleveland St., Elyria, OH 44126
27. Tom Yonushonis, Cummins Engine Company, Inc., 1900 McKinley Avenue MC: 50183, Columbus, IN 47201
28. Yuri Kalish, Detroit Diesel Corporation, 13400 Outer Drive W., Detroit, MI 48329-4001.
29. George Hansen, Detroit Diesel Corporation, 13400 Outer Drive W., Detroit, MI 48329-4001.